Published online: December 30, 2020

Original Research

Danggui Sini decoction protects against oxaliplatin-induced peripheral neuropathy in rats

Rong Ding[1,2,†], Yue Wang[3,†], Ji-Ping Zhu[4], Wu-Guang Lu[1,2], Guo-Li Wei[1,2], Zhan-Cheng Gu[5], Zhen-Tao An[6] and Jie-Ge Huo[1,2,*]

[1] *Affiliated Hospital of Integrated Traditional Chinese and Western Medicine, Nanjing University of Chinese Medicine, 210028, Nanjing, P. R. China*

[2] *Jiangsu Province Academy of Traditional Chinese Medicine, 210029, Nanjing, P. R. China*

[3] *Nanjing University of Chinese Medicine, 210023, Nanjing, P. R. China*

[4] *Affiliated Hospital of Nanjing University of Chinese Medicine, 210023, Nanjing, P. R. China*

[5] *Haimen City Hospital of Traditional Chinese Medicine, 226100, Nantong, P. R. China*

[6] *81 Hospital of People's Liberation Army, 210002, Nanjing, P. R. China*

*Correspondence: hjg16688@126.com (Jie-Ge Huo)

†These authors contributed equally.

DOI:10.31083/j.jin.2020.04.1154

The effects of *Danggui Sini* decoction on peripheral neuropathy in oxaliplatin-induced peripheral is established. The results indicated that *Danggui Sini* decoction treatment significantly reduced the current amplitude of dorsal root ganglia cells undergoing agonists stimuli compared to the model-dorsal root ganglia group ($P < 0.05$). *Danggui Sini* decoction treatment significantly inhibited the inflammatory response of dorsal root ganglia cells compared to the model-dorsal root ganglia group ($P < 0.05$). *Danggui Sini* decoction treatment significantly enhanced the amounts of Nissl bodies in dorsal root ganglia cells compared to the Model-dorsal root ganglia group ($P < 0.05$). *Danggui Sini* decoction treatment improved ultra-microstructures of dorsal root ganglia cells. In conclusion, *Danggui Sini* decoction protected against neurotoxicity of oxaliplatin-induced peripheral neuropathy in rats by suppressing inflammatory lesions, improving ultra-microstructures, and enhancing amounts of Nissl bodies.

Keywords

Oxaliplatin; peripheral neuropathy; neurotoxicity; electrophysiology

1. Introduction

Peripheral neuropathy (PN) commonly occurs post the treatment of oxaliplatin (OXAL) (Kono et al., 2015; Traina, 2017). It is also caused by diabetes, toxins, or drugs (such as chemotherapeutic drugs), burns. For diabetic peripheral neuropathy (DPN) during the diabetes process, which occurs or develops in 47% to 91% diabetes patients (Sathya et al., 2017). For patients receiving neurotoxic chemotherapy, about 30% to 40% of whom would develop chemotherapy-induced peripheral neuropathy (CIPN) (Pike et al., 2012). Meanwhile, the association between burns and PN has also been proven to occur in patients with rates ranging from 2% to 52%, according to different investigations (Strong et al., 2017). Indeed, the other conditions that cause injury to the peripheral nervous system could also cause different categories of PN (Callaghan et al., 2015).

The OXAL is a third-generation anti-tumor drug that is extensively applied for treating recurrent or advanced colorectal cancer (Engstrom et al., 2009). OXAL has been proven to be the most effective chemotherapeutic strategy for advanced or metastatic colorectal cancer (Andre et al., 2004). Therefore, chemotherapy-induced PN, has an adverse-effect post the OXAL application (Kono et al., 2015; Traina, 2017). It is characterized by hyperesthesia to cold-stimulation and could decrease the life quality of patients (Argyriou et al., 2013; Checchia et al., 2017).

Yamanouchi et al. (2017) reported that systematic inflammation contributes to the occurrence of docetaxel-induced PN. Park et al. (2013) also indicated that chemotherapy-induced peripheral neurotoxicity is associated with PN in cancer patients. The clinical symptoms, such as chronic neurotoxicity and inflammations, occur in more than 60% PN patients (Ventzel et al., 2016). The OXAL-induced PN includes plenty of severe symptoms, including numbness, sensory ataxia, and even sensations of pain, all of which would be worsen following with the continued OXAL treatment in clinical (Mizuno et al., 2016). Therefore, amelioration, inhibition or prevention of the above symptoms are critical for inhibiting the subsequent side-effects of OXAL chemotherapy.

Danggui Sini decoction (DSD), an aqueous extract of *Angelica sinensis*, *Ramulus Cinnamomi*, and *Radix Puerariae*, has been used extensively in traditional Chinese medicine (Gao et al., 2015). The previous pharmacological reports (Qian et al., 2014; Yang, 2008) illustrated that DSD plays a role in expanding blood vessels, anti-coagulation, anti-inflammation, and analgesia. Therefore, DSD is mainly used to treat coronary heart disease, ischemic vascular disorders, venous thrombosis. Moreover, DSD could also effectively inhibit oxidative stress, apoptosis and modulate mito-

Journal of Integrative Neuroscience

chondrial functions (Wolfrum et al., 2001; Yokozawa et al., 2000). We hypothesize that the DSD administration might potentiate the anti-neurotoxicity effects on peripheral neuropathy of animal models. If the hypothesis is correct, then the present study will provide an alternative anti-neurotoxic drug for treating OXAL-induced peripheral neuropathy.

2. Materials and methods

2.1 Animals

A total of 30 specific pathogen-free (SPF) Wistar rats, weighting 250-250 g (male), were purchased from Tengxin BioTech. Co. Ltd. (Chongqing, P. R. China). The rats were maintained in a 12 h/12 h light/dark cycle at 23-25 °C. The rats were freely accessed to water and standard commercial diet (CLEA Japan Inc., Shizuoka, Japan). All experiments involving rats were conducted based on Institutional Animal Care and Use Committee Guidelines of Affiliated Hospital of Integrated Traditional Chinese and Western Medicine, Nanjing, P. R. China (Approval No. AEWC-20180326-29).

2.2 Establishment of neurotoxicity rat model and grouping

A total of 24 rats were intraperitoneally injected with 4 mg/kg OXAL, according to the dosage regimen of OXAL derived in a previous study (Homles et al., 1998). The OXAL was injected into rats twice per week for 4 weeks (at day 1, day 2, day 8, day 9, day 15, day 16, day 22 and day 23, respectively). The detailed processes for establishing peripheral neuropathy rat model and sample selection were as follows: (i) intragastric administration of *Danggui Sini* decoction, (ii) intraperitoneal injection of oxaliplatin, (iii) chloral hydrate anesthesia, (iv) cardiac perfusion, (v) isolation of nerve and sample collection. Meanwhile, the dorsal root ganglia (DRG) was isolated according to the previous study reported (Gu et al., 2010). The whole experimental design and processes of this study were listed in Fig. 1.

The above 24 rat models were divided into 4 groups, including Model-DRG group (n = 6), rat model treated with low-dosage of DSD group (DSD-L-DRG group, n = 6), rat model treated with medium-dosage DSD group (DSD-M-DRG group, n = 6) and rat model treated with high-dosage DSD group (DSD-H-DRG group, n = 6). Meanwhile, the other normal 6 rats were employed as the control group (Blank-DRG group, n = 6).

2.3 Danggui Sini decoction administration

Clinically, the prescribed dosage of DSD for an adult is 54 g, and low-dosage is 0.62 g/mL, medium-dosage is 1.24 dosage g/mL, high-dosage is 2.48 g/mL (Liu et al., 2017). In this study, rats in DSD-L-DRG group (with 0.62 g/mL crude-drug), DSD-M-DRG group (with 1.24 g/ml crude-drug) and DSD-H-DRG group (with 2.48 g/mL crude-drug) were intragastrically administrated with 10 mL/kg DSD according to the above dosage of adults and a previous study reported (Liu et al., 2017), with a few modifications. The DSD was administered once daily for 4 weeks. Meanwhile, the Blank-DRG group and Model-DRG group were administrated with 0.9% NaCl at a final concentration of 10 mL/kg once daily for 4 weeks.

2.4 The dorsal root ganglia cells isolation

The rats were immobilized by intraperitoneally injected with 0.7% Choral hydrate (at a final concentration of 400 mg/kg body weight) for isolating the dorsal root ganglia for following experiments. At the end of all experiments, the mice were undergone the euthanasia by intraperitoneally injecting with pentobarbital at dosage of 120 mg/kg body weight. The dorsal root ganglia were isolated by utilizing the micro-forceps and placed in D-Hank's medium at a temperature of 4 °C to remove redundant fibroblasts and keep DRG cell viability. The dorsal root ganglia were cut into small pieces and digested with 0.03% collagenase I and 0.25% trypsin (Beyotime Biotech. Shanghai, P. R. China) at 37 °C for 5 min. Then, the isolated DRG cells were re-suspended in Dulbecco's modified eagle's medium (DMEM, Gibco BRL.Co.Ltd., Grand Island, New York, USA) complementing with 10% fetal bovine serum (FBS, Gibco BRL.Co.Ltd., Grand Island, New York, USA). The detailed processes for DRG isolation were performed according to the published study (Zhao et al., 2014).

2.5 Patch-clamp electrophysiology

To investigate the effects of DSD treatment on electrophysiological characteristics of the membrane, Patch-clamp electrophysiology was conducted in this study. In the present patch-clamp electrophysiology experiment, DRG cells were also treated with transient receptor potential vanilloid 1 (TRPV1) agonist capsaicin (at a final concentration of 1 μM) (Lin and Chen, 2015), transient receptor potential cation channel A1 (TRPA1) agonist mustard oil (at a final concentration of 100 μM) (Kistner et al., 2016) and transient receptor potential melastatin 8 (TRPM8) agonist menthol (at a final concentration of 100 μM) (Tsuzuki et al., 2004), due to the previous studies described. Briefly, the patch recordings of DRG were conducted using borosilicate glass electrodes with resistance ranging from 3 mol/LΩ to 6 mol/LΩ (A-M Systems, Sequim, WA, USA). Then, the borosilicate glass electrodes were backfilled with a saline solution composing of 10 mmol/l 2-[4-(2-Hydroxyethyl)-1-piperazinyl] ethane sulfonic acid (HEPES), 2.5 mmol/l $CaCl_2$, 10 mmol/l ethylene glycol-bis (β-aminoethyl ether)-N,N,N',N'-tetraacetic acid (EGTA), 1.0 mmol/l adenosine triphosphate, 130 mmol/l potassium gluconate, 1.0 mmol/l $MgCl_2$ and 0.3 mmol/l guanosine triphosphate. The voltage and the current recordings were captured from the isolated DRG cells by employing a patch-clamp amplifier (Mode: Axopath 200B, Axon Instruments, Foster City, CA, USA). Voltage and the current recordings were also analyzed using pClamp 10 software (Axon Instruments, Foster City, CA, USA). The other detailed processes for patch-clamp electrophysiology were conducted as the previous study described (Grabauskas et al., 2011).

2.6 Hematoxylin-eosin staining

DRG tissue was isolated according to the above methods and was fixed using 4% formaldehyde (Beyotime Biotech., Shanghai, P. R. China) in PBS solution (Beyotime Biotech). Then, the DRG tissue was simultaneously embedded with the paraffin, and the histology of DRG tissues was also simultaneously visualized with hematoxylin-eosin (HE) staining based on previously published reports (Damjanov and Andrews, 2016). The HE stained DRG tissue was captured and observed using a digital microscope (Mode: DSX110, Olympus, Tokyo, Japan). Finally, the digital graphs or electronic images were collected from the representative areas with a magnification of 100 ×. Here, the cells were counted by counting cell nuclei with a manual count method. The percent-

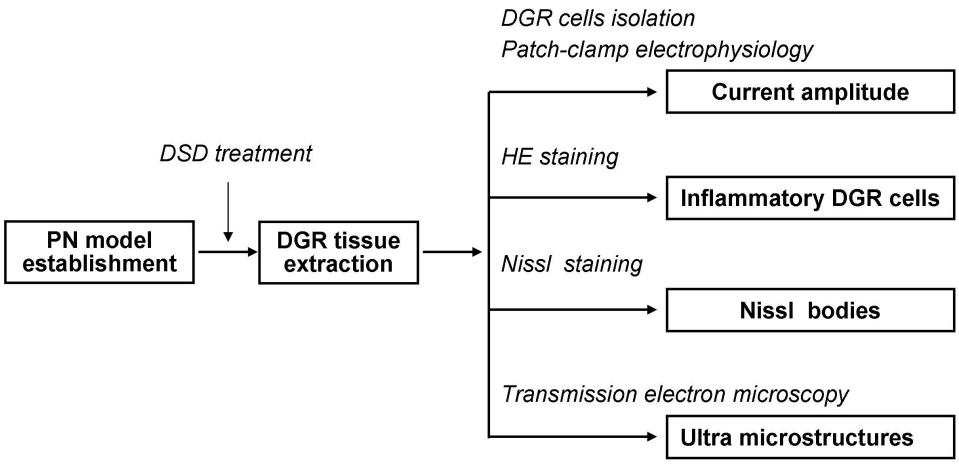

Fig. 1. The experimental design graph of the present study. The whole experimental processes mainly included "PN model establishment", "DGR tissue extraction", "evaluation of current amplitude, inflammatory DGR cells, Nissl bodies, and ultra-microstructures (using different methods)".

age of positively stained inflammatory cells (%) was represented as a ratio of the number of positive cells to the total number of cells in representative areas.

2.7 Nissl staining

The amounts of Nissl bodies represent the status of DRG cells; therefore, the Nissl bodies were evaluated in this study. Therefore, the neuronal damages of DRG tissues were simultaneously evaluated by staining with the Nissl staining method as instruction of manufacturer (Beyotime Biotech. Shanghai, P. R. China). The paraffin-embedded DRG tissues were sliced into sections with a thickness of 0.4 μm. Then, the paraffin-embedded DRG sections were deparaffinized and hydrated and stained using Nissl staining solution at 37 °C for 30 min. Finally, the DRG sections were immersed into 0.1 mol/l PBS and washed 3 times (5 min per time). In this study, the Nissl staining formed Nissl bodies (ellipsoidal or triangle corpuscle) mainly distributed in the cytoplasm of neurons and represented the normal physiological conditions of neurons. When the neurons suffering from pathological conditions, Nissl bodies might be dissolved and disappeared (Song et al., 2018). Therefore, amounts of Nissl body represented the status of cells. In this study, cells were counted by counting cell nuclei with a manual count method. The percentage of Nissl body-positive cells (%) was represented as a ratio of the number of Nissl body-positive stained cells to the total number of cells in representative areas.

2.8 Transmission electron microscopy

DRG tissue samples (size of 1 to 1.5 mm^3 pieces) were washed with phosphate-buffered saline (PBS) and fixed with 4% paraformaldehyde (Beyotime Biotech., Shanghai, P. R. China) overnight at room temperature. The pieces were washed with PBS for 5 min and fixed with 2% osmium, dehydrated in the different concentrations of acetones, including 30%, 50%, 70% combining with 2% uranyl acetate. Then, the pieces were cleared using propylene oxide and embedded in Araldite (Sigma-Aldrich, St. Louis, Missouri, USA). The pieces were cut into a series of sections (1.5 μm) and stained with 1% toluidine blue lightly. The sections were then continuously cut into ultrathin section (0.08 μm) and stained with 1% uranyl acetate and incubated with Reynold's lead citrate for 10 min. The sections were examined using a Philips TECNAI-10 transmission electron microscopy (TEM, Philips, Holland, Switzerland). The ultrathin sections were stained using the toluidine blue, and the images were captured using microscopy (Mode: BX51, Olympus, Tokyo, Japan).

2.9 Statistical analysis

SPSS 18.0 software (SPSS, Inc., Chicago, IL, USA) was used for data analysis. The measurement data were presented as mean $\pm$ standard deviation (SD). One-way ANOVA test validated by Tukey's posthoc test was employed to compare data among multiple groups. Student's *t*-test was used to compare differences between groups. $P < 0.05$ was depicted as statistical significance.

3. Results

3.1 Danggui Sini decoction treatment reduced the current amplitude of DGR cells undergoing Agonists stimuli

Patch-clamp electrophysiology results showed that the current amplitude levels of low-, medium- and the high-DSD-DGR group were significantly decreased compared to the Model-GRG group (Fig. 2A, all $P < 0.05$). Meanwhile, the current amplitude levels of DSN-L, DSD-M, GSD-H-DRG + capsaicin group were significantly decreased compared to the Model-DRG + capsaicin group (Fig. 2A, all $P < 0.05$). Meanwhile, there were no significant differences for current amplitude among all low-, medium- and high-DSD-DGR group (Fig. 2A, all $P > 0.05$).

Moreover, when treated with the other two agonists (menthol and mustard oil), the current amplitude levels of DGR cells were also significantly reduced compared to the Mode-DRG + menthol and Model-DRG + mustard oil group, respectively (Fig. 2B, all $P < 0.05$).

3.2 Danggui Sini decoction treatment inhibited the inflammatory response of DRG cells

The inflammatory conditions could reflect the peripheral neuropathy and neurotoxicity of DRG cells; therefore, HE staining was employed to examine inflammation (Fig. 3A). The results

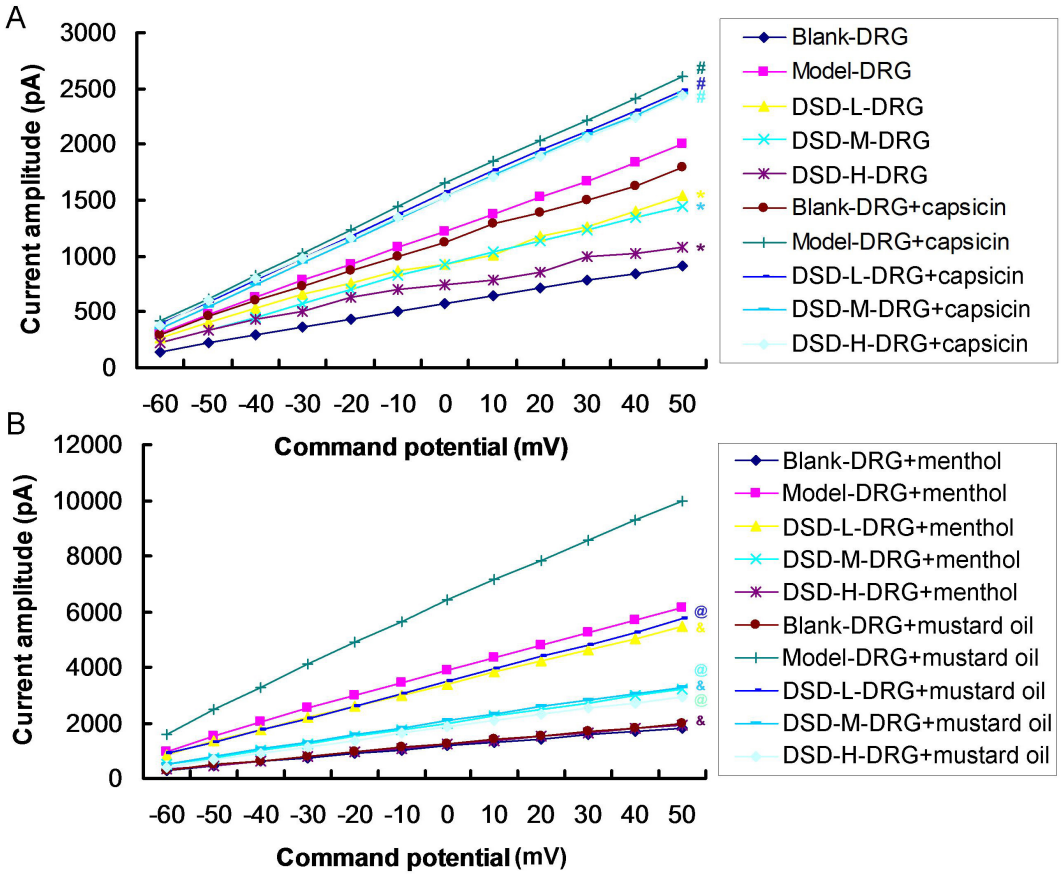

Fig. 2. Evaluation of the current amplitude using patch-clamp electrophysiology. (A) Current amplitude for the Model-DRG and Model-DRG undergoing capsaicin stimuli. (B) Current amplitude for the Model-DRG undergoing menthol and mustard oil stimuli. Low-, medium- and high-DSD-DGR treatment significantly decreased the current amplitude compared to the Model-GRG group. The current amplitude levels of DSD-L, DSD-M, GSD-H-DRG + capsaicin group were significantly decreased compared to the capsaicin administrated groups. The menthol and mustard oil administrations also illustrated the same statistical differences. The $^{*}P < 0.05$ vs. Model-DRG group. The $^{\#}P < 0.05$ vs. Model-DRG + capsaicin group. The $^{\&}P < 0.05$ vs. Model-DRG-menthol group. The $^{@}P < 0.05$ vs. Model-DRG-mustard oil group. Magnification, 100 ×.

indicated that the amounts of inflammatory cells of the Model-DRG group were significantly lower compared to the Blank-DRG group (Fig. 3B, $P < 0.05$). The DSD treatment (including lower-, medium- and higher-dosage of DSD) significantly decreased the inflammatory cell amounts compared to the Model-DRG group (Fig. 3B, $P < 0.05$). Moreover, there were no remarkable differences for amounts of inflammatory cells among all low-, medium- and high-DSD-DGR group (Fig. 3B, all $P > 0.05$).

3.3 Danggui Sini decoction treatment enhanced amounts of Nissl bodies of DRG cells

The Nissl body staining results showed that, in the Model-DRG group, there were fewer Nissl bodies illustrating with damaged morphology of Nissl bodies (Fig. 4A). Meanwhile, there even more Nissl bodies were illustrating typical ellipsoidal or triangle corpuscle morphologies (Fig. 4A). The results indicated that amounts of Nissl bodies in Model-DGR group were significantly decreased compared to Blank-DRG group (Fig. 4B, $P < 0.05$). Meanwhile, the amounts of Nissl bodies in DSD treated groups (lower-, medium- and higher-DSD) were significantly higher compared to the Model-DRG group (Fig. 4B, $P < 0.05$). Furthermore, the amounts of Nissl bodies were also increased following the increased dosage of DSD (Fig. 4B). Meanwhile, Nissl bodies in Model-M-DGR and Model-H-DGR group were higher remarkably compared to that in the Model-L-DGR group (Fig. 4B, $P < 0.05$). However, there were no significant differences for Nissl bodies between Model-M-DGR and Model-H-DGR group (Fig. 4B, $P > 0.05$).

3.4 Danggui Sini decoction treatment improved ultra-microstructures of DRG cells

According to the electron microscopy findings, there were typical ultra-microstructures of normal neurons (such as well-developed Golgi apparatus, well-structured mitochondria) in the Blank-DRG group. However, plenty of ultra-microstructures were damaged in the Model-DRG group (Fig. 5). What's most important is that the DSD treatment improved the ultra-microstructures of DRG cells (Fig. 5). Among all three dosages of DSD, ultra-microstructures were improved following the increased concentrations of DSD (Fig. 5). Furthermore, there were no obvious differences for ultra-microstructures among all three DSD treated groups (Fig. 5).

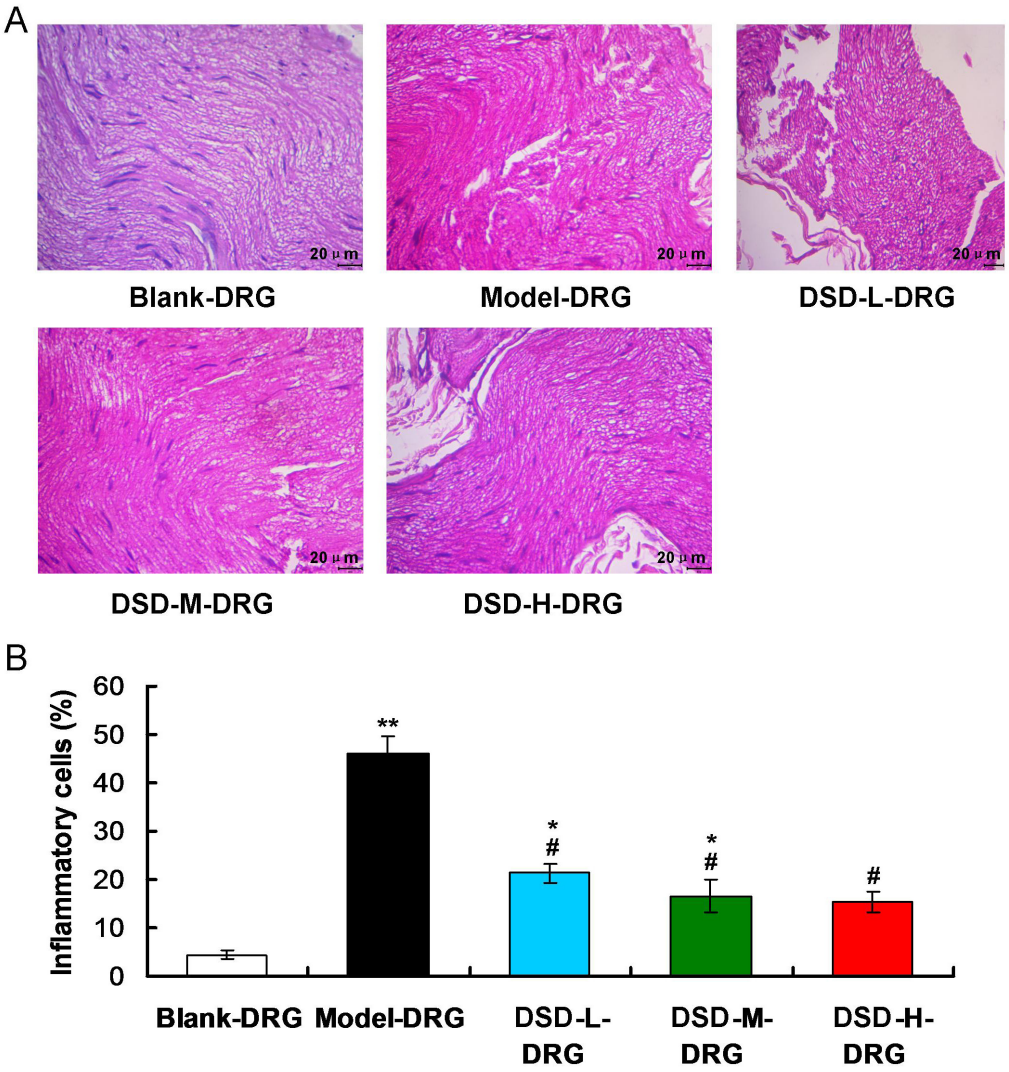

Fig. 3. Examination for the inflammatory response in DRG tissue using HE staining (n = 6 rats in each group). (A) Images of HE staining in different groups. (B) Statistical analysis for the HE staining of inflammation. The model-DRG group illustrated higher amounts of inflammatory cells compared to the Blank-DRG group, while DSD treatment decreased inflammatory cell amounts. For every group, at least 12 sections (2 sections per rat) were from rats that were used for the analysis. $^{*}P < 0.05$, $^{**}P < 0.01$ vs. Blank-DRG group, $^{\#}P < 0.05$ vs. Model-DRG group.

4. Discussion

We employed an effective Chinese Medicine, DSD, for treating oxaliplatin-induced side-effects in DRG cells. Clinically, the oxaliplatin-induced side-effects mainly include electrophysiological characteristic changes, inflammatory response, Nissl body depletion, and damaged ultra-microstructures, all of which are associated with peripheral neuropathy or neurotoxicity (Coriat et al., 2014; Kono et al., 2015; Naderali et al., 2018). However, all of these side-effects always occur in patients suffering from cancers and undergoing treatment of OXAL. Therefore, the novel discovered DSD might provide a promising or potential basis for OXAL-induced side-effects or complications in clinical.

Liu et al. (2017) administrated DSD at a dosage of 25-100 mg/kg for 10 days. However, in this study, the above regimen has not been illustrated the obvious effects of GDGN. Therefore, we administrated the DSD at 10 mg/kg daily for 4 weeks. In this study, the electrophysiological data of the Model-DRG group showed the abnormal current amplitudes that probably damage the physiological functions of DRG cells. The varied or aberrant currents have been illustrated in different sizes of DRG neurons (Scroggs et al., 1994). DSN treatment resulted in the enhanced excitability and reduced current amplitude of DGR cells undergoing agonists stimuli (Than et al., 2013), such as TRPV1 agonist, capsaicin (Lin and Chen, 2015), TRPM8 agonist, menthol (Tsuzuki et al., 2004) and TRPA1 agonist, mustard oil (Kistner et al., 2016). The TRPM8 is a sensory molecule expressing on the subpopulation of the primary afferent neurons and can be activated by menthol (McKemy et al., 2002). TRPV1 normally selectively expresses in small-medium DRG neurons and up-regulates in uninjured sensory neurons post the partial nerve injury (Kim et al., 2008). TRPA1, as a cold-sensor, plays roles in pain and inflammation of DRG neurons (Kistner et al., 2016). All of the above TRPM8, TRPV1 and TRPA1 molecules could modulate the intracellular Ca^{2+} levels (or voltage-gated Ca^{2+}channels), involve multiple intracellular re-

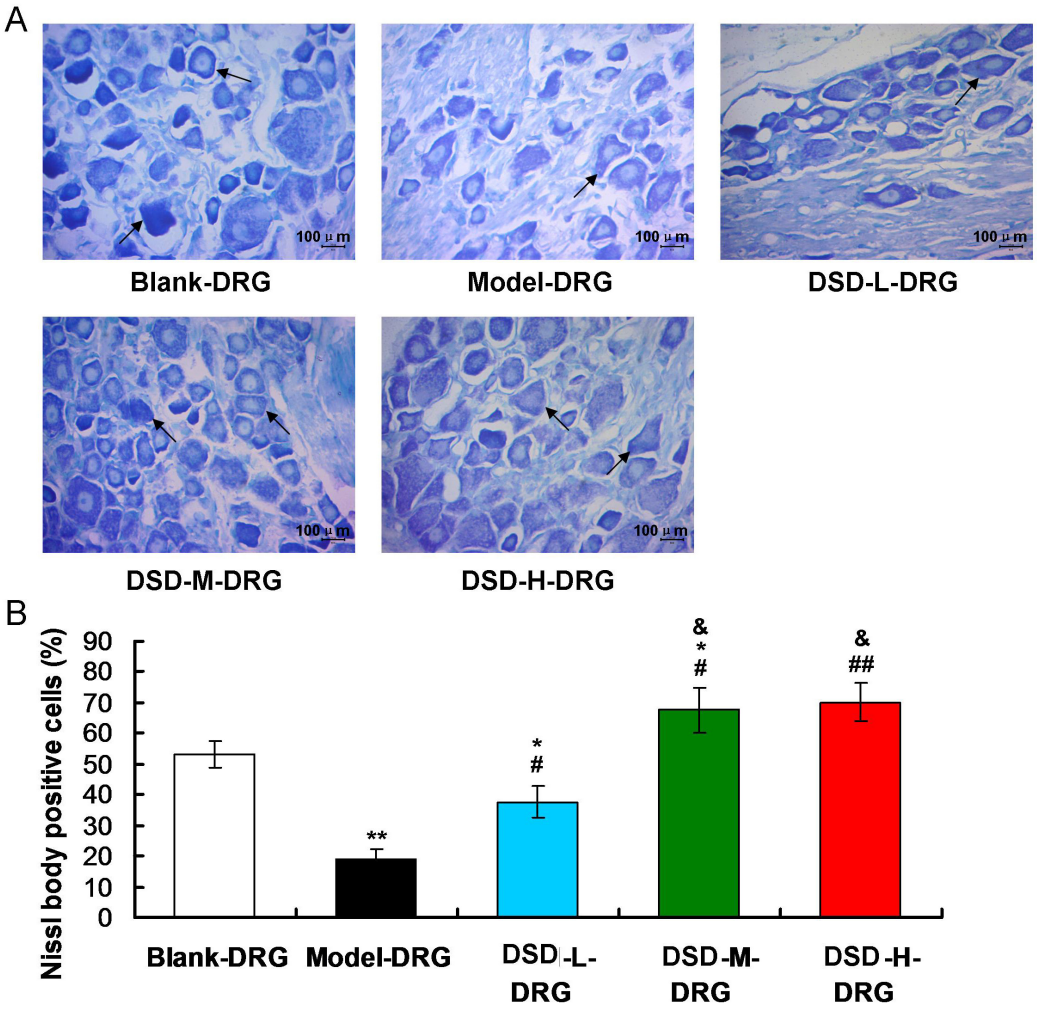

Fig. 4. Nissl body identification in DRG tissue using Nissl staining method (n = 6 in each group). (A) Graphs for the Nissl staining positive Nissl bodies. (B) Statistical analysis for the Nissl bodies. The black arrows represent the Nissl bodies. The model-DRG group showed lower amounts of Nissl bodies compared to the Blank-DRG group, while DSD treatment enhanced Nissl bodies of DRG cells. For every group, at least 12 sections (2 sections per rat) were from rats that were used for the analysis. $^{*}P < 0.05$, $^{**}P < 0.01$ vs. Blank-DRG group, $^{\#}P < 0.05$, $^{\#\#}P < 0.01$ vs. Model-DRG group.$^{\&}P < 0.05$ vs. Model-L-DRG group.

sponses, and further contribute to intermediately adapting currents (Brierley et al., 2011; Kistner et al., 2016; McKemy et al., 2002).

Choi et al. (2006) also reported that the electrogenesis of DRG neurons is correlated with the reduced current amplitude, which could reflect the physiological functions of DRG cells. Our results indicated that the low-, medium- and high-DSD-DGR treatment, as well as DGR plus TRPM8, TRPV1 and TRPA1 agonists, significantly reduced current amplitude. These results suggest that the DSD treatment remarkably improved the physiological functions of DRG cells by reducing the current amplitudes.

Chen et al. (2014) and Yamanouchi et al. (2017) reported that inflammation is associated with the injury or damage of neurons. Therefore, HE staining was used to observe the inflammatory response in this study. Our results illustrated that DSD treatment significantly decreased the formation of inflammatory lesions in DRG tissues, with a dose-dependent efficacy. Therefore, we speculated that the effective inhibition of inflammation using DSD could result in the suppression of neuronal damages. This result suggests that the DSD remarkably alleviates the pathogenesis of peripheral neuropathy by inhibiting inflammation in DRG tissues. The functional mechanism of DSD is consistent with the report of a previous study (Yamanouchi et al., 2017).

In this study, we also observed Nissl bodies in DRG cells, which are the biomarker for the normal morphology of neurons (Niu et al., 2015). Our data showed that the DSD treatment enhanced the amounts of Nissl bodies and improved the morphology of DRG cells. Lin et al. (2017) reported that the DRG cells in painful diabetic neuropathy significantly reduced amounts of Nissl bodies. Therefore, the amounts of Nissl bodies could reflect the proliferative status of DRG cells. In this study, we confirmed that the DSD could promote DRG cell viability by improving the morphology of Nissl bodies.

Moreover, ultra-microstructures of DRG cells were also evaluated. The results showed that DSD could improve the dam-

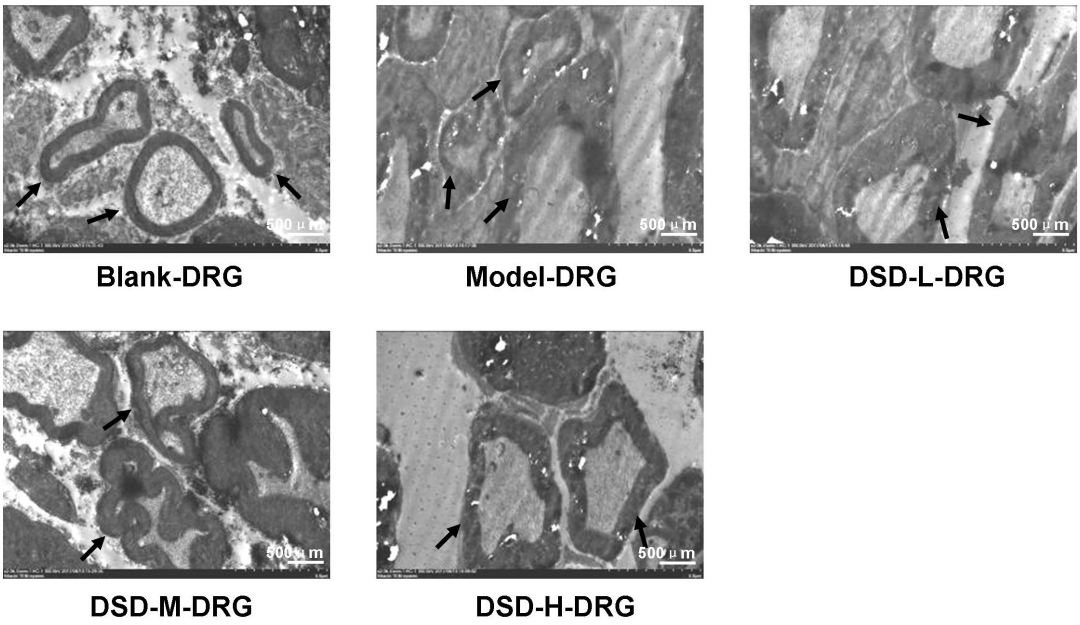

Fig. 5. Evaluation of the ultra-microstructures of DRG tissue using transmission electron microscopy (n = 6 in each group). The images showed that the DSD treatment improved the ultra-microstructures of DRG cells. Magnification, 2000 ×. The black arrows represented the Golgi apparatus and/or mitochondria.

aged ultra-microstructures of DRG cells to be well-developed morphologies (Kerchner et al., 2012). This result suggests that DSD treatment effectively inhibits the OXAL-induced ultra-microstructure changes of DRG. The findings of ultra-microstructures in DRG cells undergoing DSD treatment are consistent with HE staining and Nissl staining results, all of which are inclined to the improvements of DRG cells.

In conclusion, DSD treatment reduced the current amplitude of DGR cells undergoing Agonists stimuli and inhibited the inflammatory response and enhanced the amounts of Nissl bodies in DRG cells. DSD treatment also improved the ultra-microstructures of DRG cells, consistent with our hypothesis. Finally, DSD did protect against the neurotoxicity of OXAL-induced peripheral neuropathy in the rat model by suppressing inflammatory lesions, improving ultra-microstructures, and enhancing amounts of Nissl bodies.

Abbreviations

CIPN: chemotherapy-induced peripheral neuropathy; DSD: *Danggui Sini* decoction; DMEM: Dulbecco's modified eagle's medium; DRG: dorsal root ganglia; EGTA: ethylene glycol-bis (β-aminoethyl ether)-N,N,N',N'-tetraacetic acid; FBS: fetal bovine serum; HE: Hematoxylin-eosin; HEPES: 2-[4-(2-Hydroxyethyl)-1-piperazinyl] ethane sulfonic acid; OXAL: oxaliplatin; PBS: phosphate-buffered saline; PN: Peripheral neuropathy; SPF: specific pathogen-free; TEM: transmission electron microscopy; TRPA1: transient receptor potential cation channel A1; TRPM8: transient receptor potential melastatin 8; TRPV1: transient receptor potential vanilloid 1.

Author contributions

RD and JGH designed the research study. RD, YW, JPZ, WGL, and GLW performed the research. ZCG made the statistical analysis. ZTA conducted the literature review.

Ethics approval and consent to participate

The present study was conducted according to the Guidance of Care and Use of Laboratory Animals of the National Institute of Health (NIH). All of the animal experiments were approved by the Ethics Committee of Nanjing University of Chinese Medicine, Nanjing, P. R. China. All experiments involving rats were conducted based on Institutional Animal Care and Use Committee Guidelines of Affiliated Hospital of Integrated Traditional Chinese and Western Medicine, Nanjing, P. R. China (Approval No. AEWC-20180326-29).

Acknowledgment

This study was granted by the National natural science foundation of the People's Republic of China (Grant No. 81503568), the National natural science foundation of Jiangsu Province (Grant No. BK20151049) and Bureau of Traditional Chinese Medicine of Jiangsu Province of China (Grant No. YB2015035).

Conflict of Interest

The authors declare no competing financial or commercial interests in this manuscript.

Submitted: August 17, 2019
Revised: October 30, 2019
Accepted: November 04, 2019
Published: December 30, 2020

References

Andre, T., Boni, C., Mounedji-Boudiaf, L., Navarro, M., Tabernero, J., Hichish, T., Topham, C., Zaninelli, M., Clingan, P., Bridgewater, J., Tabah-Fisch, I. and de Gramont, A. (2004) Oxaliplatin, Fluorouracil, and Leucovorin as adjuvant treatment for colon cancer. *The New England Journal of Medicine* **350**, 2343-2351.

Argyriou, A. A., Cavaletti, G., Briani, C., Velasco, R., Bruna, J., Campagnolo, M., Alberti, P., Bergamo, F., Cortinovis, D., Cazzaniga, M., Santos, C., Papadimitriou, K. and Kalofonos, H. P. (2013) Clinical pattern and associations of Oxaliplatin acute neurotoxicity: a prospective study in 170 patients with colorectal cancer. *Cancer* **119**, 438-444.

Bao, J. W., Sun, B., Ma, P. P., Gai, Y. S., Sun, W. Z., Yu, H. Q. and Li, J. (2018) Rosuvastatin inhibits inflammatory response and resists fibrosis after myocardial infarction. *European Review Medical and Pharmacological Science* **22**, 238-245.

Brierley, S. M., Castro, J., Harrington, A. M., Hughes, P. A., Page, A. J., Rychkov, G. Y. and Blackshaw, L. A. (2011) TRPA1 contributes to specific mechanically activated currents and sensory neuron mechanical hypersensitivity. *The Journal of Physiology* **589**, 3575-3593.

Callaghan, B. C., Price, R. S., Chen, K. S. and Feldman, E. L. (2015) The importance of rare subtypes in diagnosis and treatment of peripheral neuropathy: a review. *JAMA Neurology* **72**, 1510-1518.

Checchia, G. A., Letizia Mauro, G., Morico, G., Oriente, A., Lisi, C., Polimeni, V., Lucia, M., Ranieri, M. and Management of Peripheral Neuropathies Study Group. (2017) Observational multicentric study on chronic sciatic pain: clinical data from 44 Italian centers. *European Review Medical and Pharmacological Science* **21**, 1653-1664.

Chen, C. C., Hung, T. H., Lee, C. Y., Wang, L. F., Wu, C. H., Ke, C. H. and Chen, S. F. (2014) Berberine protects against neuronal damage via suppression of glia-mediated inflammation in traumatic brain injury. *PLoS One* **9**, e115694.

Choi, J. S., Hudmon, A., Waxman, S. G. and Dib-Hajj, S. D. (2006) Calmodulin regulates current density and frequency-dependent inhibition of sodium channel Nav1.8 in DRG neurons. *Journal of Neurophysiology* **96**, 97-108.

Coriat, R., Alexandre, J., Nicco, C., Quinquis, L., Benoit, E., Chereau, C., Lemarechal, H., Mir, O., Borderie, D., Treluyer, J. M., Weill, B., Coste, J., Goldwasser, F. and Batteux, F. (2014) Treatment of Oxaliplatin-induced peripheral neuropathy by intravenous Mangafodipir. *Journal of Clinical Investigation* **124**, 262-272.

Damjanov, I. and Andrews, P. W. (2016) Teratomas produced from human pluripotent stem cells xenografted into immunodeficient mice, a histopathology atlas. *International Journal of Developmental Biology* **60**, 337-419.

Engstrom, P. F., Arnoletti, J. P., Benson, A. B., Chen, Y. J., Choti, M. A., Cooper, H. S., Covey, A., Dilawari, R. A., Early, D. S. and Enzinger, P. C. (2009) National comprehensive cancer network. NCCN clinical practice guidelines in oncology: colon cancer. *Journal of the National Comprehensive Cancer Network* **7**, 778-831.

Gao, Y., Hao, J., Zhang, H., Qian, G., Jiang, R., Hu, J., Wang, J., Lei, Z. and Zhao, G. (2015) Protective effect of the combinations of glycyrrhizic, Ferulic and cinnamic acid prereatment on myocardial ischemia-reperfusion injury in rats. *Experimental and Therapeutic Medicine* **9**, 435-445.

Grabauskas, G., Heldsinger, A., Wu, X., Xu, D., Zhou, S. and Owyang, C. (2011) Diabetic visceral hypersensitivity is associated with activation of mitogen-activated kinase in rat dorsal root ganglia. *Diabetes* **60**, 1743-1751.

Gu, Y., Hu, H., Liu, J., Ding, F. and Gu, X. (2010) Isolation and differentiation of neural stem/progenitor cells from fetal rat dorsal root ganglia. *Science China Life Sciences* **53**, 1057-1064.

Homles, J., Stanko, J., Varchenko, M., Ding, H., Madden, V. J., Bagnell, C. R., Wyrick, S. D. and Chaney, S. G. (1998) Comparative neurotoxicity of Oxaliplatin, Cisplatin and Ormaplatin in a Wistar rat model. *Toxicological Sciences* **46**, 342-351.

Kerchner, G. A., Deutsch, G. K., Zeineh, M., Dougherty, R. F., Saranathan, M. and Rutt, B. K. (2012) Hippocampal CA1 apical neuropil atrophy and memory performance in Alzheimer's Disease. *Neuroimage* **63**, 194-202.

Kim, H. Y., Park, C. K., Cho, I. H., Jung, S. J., Kim, J. S. and Oh, S. B. (2008) Differential changes in TRPV1 expression after trigeminal sensory nerve injury. *The Journal of Pain* **9**, 280-288.

Kistner, K., Siklosi, N., Babes, A., Khalil, M., Selescu, T., Zimmermann, K., Wirtz, S., Becker, C., Neurath, M. F., Reeh, P. W. and Engel, M. A. (2016) Systemic desensitization through TRPA1 channels by Capsazepine and mustard oil, a novel strategy against inflammation and pain. *Scientific Reports* **6**, 28621.

Kono, T., Suzuki, Y., Mizuno, K., Miyagi, C., Omiya, Y., Sekine, H., Mizuhara, Y., Miyano, K., Kase, Y. and Uezono, Y. (2015) Preventive effect of oral goshajinkigan on chronic Oxaliplatin-induced hypoesthesia in rats. *Scientific Reports* **5**, 16078.

Lin, J. Y., Huang, X. L., Chen, L., Yang, Z. W., Lin, J., Huang, S. and Peng, B. (2017) Stereological study on the number of synapses in the rat spinal dorsal horn with painful diabetic neuropathy induced by streptozotocin. *Neuroreport* **28**, 319-324.

Lin, Y. W. and Chen, C. C. (2015) Electrophysiological characteristics of IB4-negative TRPV1-expressing muscle afferent DRG neurons. *Biophysics (Nagoya-shi)* **11**, 9-16. (In Japanese)

Liu, M., Qiang, Q. H., Ling, Q., Yu, C. X., Li, X., Liu, S. and Yang, S. (2017) Effects of *Danggui Sini* decoction on neuropathic pain: experimental studies and clinical pharmacological significance of inhibiting glial activation and proinflamatory cytokines in the spinal cord. *International Journal of Clinical Pharmacology and Therapeutics* **55**, 453-464.

McKemy, D. D., Neuhausser, W. M. and Julius, D. (2002) Identification of a cold receptor reveals a general for TRP channels in thermosensation. *Nature* **416**, 52-58.

Mizuno, K., Shibata, K., Komatsu, R., Omiya, Y., Kase, Y. and Koizumi, S. (2016) An effective therapeutic approach for Oxaliplatin-induced peripheral neuropathy using a combination therapy with goshajinkigan and bushi. *Cancer Biology and Therapy* **17**, 1206-1212.

Naderali, E., Nikbakht, F., Ofogh, S. N. and Rasoolijazi, H. (2018) The role of rosemary extract in degeneration of hippocampal neurons induced by kainic acid in the rat: a behavioral and histochemical approach. *Journal of Integrative Neuroscience* **17**, 19-25.

Niu, J., Li, C., Wu, H., Feng, X., Su, Q., Li, S., Zhang, L., Yew, D. T., Cho, E. Y. and Sha, O. (2015) Propidium iodide (PI) stains Nissl bodies and may serve as a quick marker for total neuronal cell count. *Acta Histochemica* **117**, 182-187.

Park, S. B., Goldstein, D., Krishnan, A. V., Lin, C. S., Friedlander, M. L., Cassidy, J., Koltzenburg, M. and Kiernan, M. C. (2013) Chemotherapy-induced peripheral neurotoxicity: a critical analysis. *CA: A Cancer Journal for Clinicians* **63**, 419-437.

Pasetto, L. M., D'Andrea, M. R., Rossi, E. and Monfardini, S. (2006) Oxaliplatin-related neurotoxicity: how and why? *Critical Reviews in Oncology Hematology* **59**, 159-168.

Pike, C. T., Birnbaum, H. G., Muehlenbein, C. E., Pohl, G. M. and Natale, R. B. (2012) Healthcare costs and workloss of patients with chemotherapy-associated peripheral neuropathy in breast, ovarian, head and neck, and nonsmall cell lung cancer. *Chemotherapy Research Practice* **2012**, 913848.

Qian, G. Q., Peng, X., Cai, C. and Zhao, G. P. (2014) Effect on eNOS/NO pathway in MIRI rats with preconditioning of GFPC from Dang Gui Si Ni decoction. *Pharmacognosy Research* **6**, 133-137.

Sathya, G. R., Krishnamurthy, N., Veliath, S., Arulneyam, J. and Venkatachalam, J. (2017) F wave index: a diagnostic tool for peripheral neuropathy. *Indian Journal of Medical Research* **145**, 353-357.

Scroggs, R. S., Todorovic, S. M., Anderson, E. G. and Fox, A. P. (1994) Variation in IH, IR, and ILEAK between acutely isolated adult rat dorsal root ganglion neurons of different size. *Journal of Neurophysiology* **71**, 271-279.

Song, Y., Zhong, M. and Cai, F. C. (2018) Oxcarbazepine causes neurocyte apoptosis and developing brain damage by triggering Bax/Bcl-2 signaling pathway mediated caspase 3 activation in neonatal rats. *European Review for Medical and Pharmacological Sciences* **22**, 250-261.

Strong, A. L., Agarwal, S., Cederna, P. S. and Levi, B. (2017) Peripheral neuropathy and nerve compression syndromes in burns. *Clinics in Plastic Surgery* **44**, 793-803.

Than, J. Y., Li, L., Hasan, R. and Zhang, X. (2013) Excitation and modulation of TRPA1, TRPV1 and TRPM8 channel-expressing sensory neurons by the pruritogen chloroquine. *Journal of Biological Chemistry* **288**, 12818-12827.

Traina, G. (2017) Mast cells in the brain, old cells, new target. *Journal of Integrative Neuroscience* **16**, S69-S83.

Tsuzuki, K., Xing, H., Ling, J. and Gu, J. G. (2004) Menthol-induced Ca^{2+} release from presynaptic Ca^{2+} stores potentiates sensory synaptic transmission. *Journal of Neuroscience* **24**, 762-771.

Ventzel, L., Jensen, A. B., Jensen, A. R., Jensen, T. S. and Finnerup, N. B. (2016) Chemotherapy-induced pain and neuropathy: a prospective study in patients treated with adjuvant Oxaliplatin or Docetaxel. *Pain* **157**, 560-568.

Wolfrum, S., Richardt, G., Dominiak, P., Katus, H. A. and Dendorfer, A. (2001) Apstatin, a selective inhibitor of aminopeptidase P, reduces myocardial infarct size by a kinin-dependent pathway. *British Journal of Pharmacology* **134**, 370-374.

Yamanouchi, K., Kuba, S., Sakimura, C., Morita, M., Kanetaka, K., Kobayashi, K., Takatsuki, M., Hayashida, N. and Eguchi, S. (2017) The relationship between peripheral neuropathy induced by Docetaxel and systemic inflammation-based parameters in patients with breast cancer. *Anticancer Research* **37**, 6947-6951.

Yang, J. (2008) Advance in the clinical application of *Danggui Sini* decoction in recent five years. *Clinical Journal Traditional Chinese Medicine* **20**, 538-540.

Yokozawa, T., Liu, Z. W. and Chen, C. P. (2000) Protective effects of glycyrrhiza extract and its compounds in a renal hypoxia (ischemia)-reoxygenation model. *Phytomedicine* **6**, 439-445.

Zhao, L., Qu, W., Wu, Y., Ma, H. and Jiang, H. (2014) Dorsal root ganglion-derived Schwann cells combined with poly (lactic-co-glycolic acid)/chitosan conduits for the repair of sciatic nerve defects in rats. *Neural Regeneration Research* **9**, 1961-1967.